Sensors & Transducers, Vol. 229, Issue 1, January 2019, pp. 55-60

Sensors & Transducers

Published by IFSA Publishing, S. L., 2019

http://www.sensorsportal.com

Sensitivity Enhancement of a Self-Mixing Laser Diode Sensor by Using a Dual-cavity Configuration

Yuxi Ruan, Bin Liu, Yanguang Yu, Jiangtao Xi, Qinghua Guo, Jun Tong

School of Electrical, Computer and Telecommunications Engineering, University of Wollongong, Northfields Ave, Wollongong, NSW, 2522, Australia

Tel.: +61 4221 8187

E-mail: yanguang@uow.edu.au

Received: 30 November 2018 /Accepted: 31 December 2018 /Published: 31 January 2019

Abstract: When a part of light emitted by a laser is back-reflected or back-scattered from an external target and re-enters the laser cavity, the laser output power will be modulated. This is called Self-Mixing Effect (SME), which is a universal phenomenon occurring in lasers regardless of type. For SME based laser sensing system, a laser diode is usually employed to make a compact sensing system due to its small size. The laser diode in this case is also called Self-Mixing Laser Diode (SMLD). In some practical cases, a target surface has a very low reflectivity and thus not able to provide enough high feedback light to the laser diode. In this case, the observed sensing signal from the SMLD sensor is blurred and sensing sensitivity is degraded. To improve the sensing ability, we propose to apply a pre-feedback to the SMLD sensor. Investigation from both simulation and experiments are conducted to verify the proposed design. The results show that a proper pre-feedback can greatly enhance the sensing performance for a SMLD sensor.

Keywords: Self-mixing interferometry, Optical feedback, Laser diode.

1. Introduction

As a promising non-contact sensing technology, Self-Mixing Interferometry (SMI) has attracted much attention of researchers in recent decades. The SMI is based on the Self-Mixing Effect (SME) that occurs when a fraction of light back-reflected or back-scattered by an external target reentering the laser inside cavity [1-3]. In this case, both the laser output power and frequency are modulated. A typical Self-Mixing Laser Diode (SMLD) sensor consists of laser diode (LD), a photodiode (PD) packaged in the rear of the LD, a lens and external target, as shown in Fig. 1. As a minimum part-count scheme, various SMI-based applications have been developed in the industrial and laboratory environment, such as measurement of displacement [1, 4-7], velocity [8-9], vibration [10-11], alpha factor [12-14], thickness [15], refraction index [16], mechanical resonance [17], and imaging [18-19] material parameters measurement [20], acoustic detection [21], biomedical applications [22], etc.

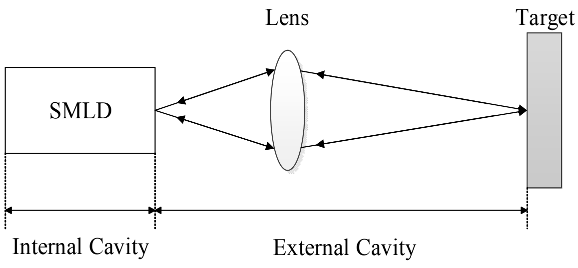

Fig. 1. Schemaic configuration of an SMI.

In some practical cases, a target surface has a very low reflectivity and thus not able to provide enough high feedback light to the LD. In this case, the observed sensing SMI signal from the SMLD sensor is blurred and sensing sensitivity is degraded.

In this work, we propose to apply a pre-feedback to the SMLD sensor to improve the system sensitivity. We firstly introduced a mathematic model for the SMLD sensor. Then, using MATLAB simulation to verify the influence on the SMLD sensor performance from the pre-feedback strength and the position of pre-feedback target. Lastly, an experimental setup is built for further verifying the proposed method.

2. Theory and Simulations

The dynamics of an SMLD sensor can be described by the well-known Lang and Kobayashi (L-K) equations [23] shown as Eq. (1) - Eq. (3). The equations state a relationship between the three variables, electric field amplitude $E(t)$, electric field phase $\phi(t)$, carrier density $N(t)$ with other parameters that are associated with the LD.

$$\frac{dE(t)}{dt} = \frac{1}{2}\left\{G\left[N(t),E(t)\right] - \frac{1}{\tau_p}\right\}E(t) + \frac{\kappa}{\tau_{in}} \cdot E(t-\tau)\cdot\cos\left[\omega_0\tau + \phi(t) - \phi(t-\tau)\right], \quad (1)$$

$$\frac{d\phi(t)}{dt} = \frac{1}{2}\alpha\left\{G\left[N(t),E(t)\right] - \frac{1}{\tau_p}\right\} - \frac{\kappa}{\tau_{in}} \cdot \frac{E(t-\tau)}{E(t)}\cdot\sin\left[\omega_0\tau + \phi(t) - \phi(t-\tau)\right], \quad (2)$$

$$\frac{dN(t)}{dt} = J - \frac{N(t)}{\tau_s} - G\left[N(t),E(t)\right]E^2(t), \quad (3)$$

$G\left[N(t),E(t)\right] = G_N\left[N(t) - N_0\right]\left[1 - \varepsilon\Gamma E^2(t)\right]$ is the modal gain per unit time, the nonlinear gain is ignored, Therefore, $G\left[N(t),E(t)\right] = G_N(N_s - N_0)$. The physical meanings of the symbols in Eq. (1) - Eq. (3) and the values of the parameters are shown in Table 1.

A pre-feedback applied to a SMLD sensor can be provided by a mirror surface. In this case, a SMLD sensor will have two targets and formed two external cavities. A SMI system with pre-feedback is shown in Fig. 2. Hence, the L-K equations can be modified as Eq. (4) - Eq. (6).

Note that the symbols with subscript '1' is referring to the measured target (Target-1) and '2' is referring to the target used to provide the pre-feedback (Target-2). The SMI signal waveform can be observed by solving the LK equations for $E^2(t)$.

$$\frac{dE(t)}{dt} = \frac{1}{2}\left\{G\left[N(t),E(t)\right] - \frac{1}{\tau_p}\right\}E(t) + \frac{\kappa_1}{\tau_{in}} \cdot E(t-\tau_1)\cdot\cos\left[\omega_0\tau_1 + \phi(t) - \phi(t-\tau_1)\right] + \frac{\kappa_2}{\tau_{in}} \cdot E(t-\tau_2)\cdot\cos\left[\omega_0\tau_2 + \phi(t) - \phi(t-\tau_2)\right], \quad (4)$$

$$\frac{d\phi(t)}{dt} = \frac{1}{2}\alpha\left\{G\left[N(t),E(t)\right] - \frac{1}{\tau_p}\right\} - \frac{\kappa_1}{\tau_{in}} \cdot \frac{E(t-\tau_1)}{E(t)}\cdot\sin\left[\omega_0\tau_1 + \phi(t) - \phi(t-\tau_1)\right] - \frac{\kappa_2}{\tau_{in}} \cdot \frac{E(t-\tau_2)}{E(t)}\cdot\sin\left[\omega_0\tau_2 + \phi(t) - \phi(t-\tau_2)\right], \quad (5)$$

$$\frac{dN(t)}{dt} = J - \frac{N_s}{\tau_s} - G_N(N_s - N_0)E^2(t) \quad (6)$$

Table 1. Physical meanings and values of the parameters in LK equations.

Symbol	Physical Meaning	Value
G_N	Modal gain coefficient	$8.1\times10^{-13} m^3 s^{-1}$
N_0	Carrier density at transparency	$1.1\times10^{24} m^{-3}$
ε	Nonlinear gain compression coefficient	$2.5\times10^{-23} m^3$
Γ	Confinement factor	0
τ_p	Photon life time	$2.0\times10^{-12} s$
τ_{in}	Internal cavity round-trip time	$8.0\times10^{-12} s$
τ_s	Carrier life time	$2.0\times10^{-9} s$
κ	Feedback strength	
τ	External cavity round trip time, $\tau = 2L/c$, where L is external cavity length, c is speed of light	
ω_0	Angular frequency of solitary laser	
α	Line-width enhancement factor	3.0
J	Injection current density	

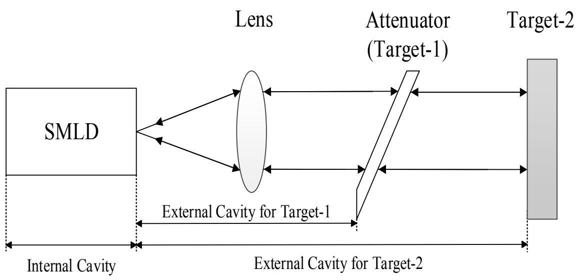

Fig. 2. Schematic configuration of an SMI with pre-feedback.

2.1. Simulation Verification on Pre-feedback Strength Influence

We implemented the LK equations Eq. (4) - Eq. (6) in MATLAB. The LD parameter values are given in Table 1. We set the LD wavelength as $\lambda = 830\times10^{-9}$ m . Target 1 has the feedback strength $\kappa_1 = 0.00011$, the intial external cavity length is $L_1 = 0.35\text{m}$. Target 2 has the feedback strength $\kappa_2 = 0.0004$, the initial external cavity length is $L_2 = 0.16$ m . We define the magnified factor is the ratio of SMI waveform magnitude with pre-feedback divided by its magnitude without pre-feedback. We tested different κ_2 while all other parameters remain unchanged. Fig. 3 shows the SMI waveforms when $\kappa_2 = 0.0004$, the peak to peak value for the no pre-feedback waveform is 0.8347 and with the pre-feedback is 0.9533. The magnified factor is 1.14.

Fig. 4 shows the SMI waveforms when $\kappa_2 = 0.0011$, the peak to peak value for the no pre-feedback remain unchanged and with the pre-feedback is 1.1862. The magnified factor is 1.42.

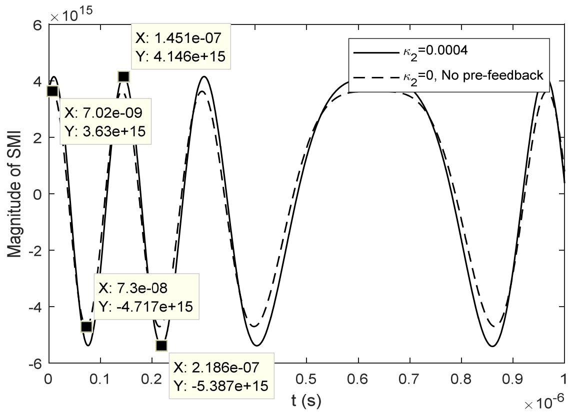

Fig. 3. SMI pre-feedback when $\kappa_2 = 0.0004$ vs SMI without pre-feedback.

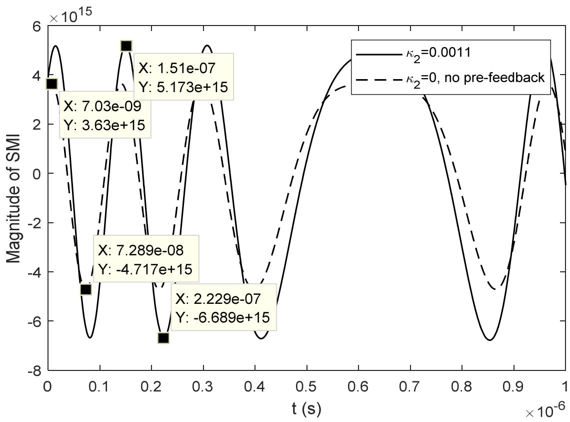

Fig. 4. SMI pre-feedback when $\kappa_2 = 0.0011$ vs SMI without pre-feedback.

Fig. 5 shows the SMI waveforms when $\kappa_2 = 0.0018$, the peak to peak value for the pre-feedback is 1.5228. The magnified factor is 1.82.

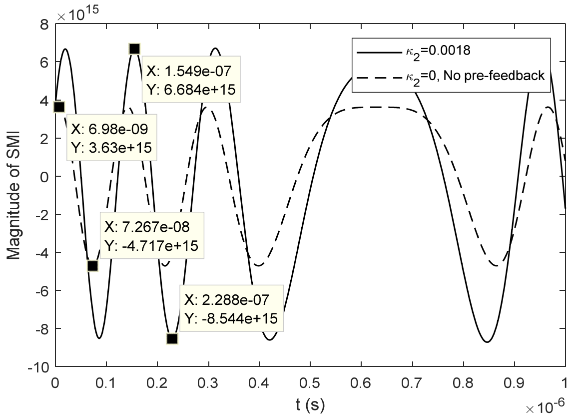

Fig. 5. SMI pre-feedback when $\kappa_2 = 0.0018$ vs SMI without pre-feedback.

2.2. Simulation Verification on Pre-feedback Target Location Influence

We then invesitage the influence of the pre-feedback target location on the SMI waveform. We maintain Target-1 feedback strength as $\kappa_1 = 0.00011$. We set Target-2 has a feedback strength $\kappa_2 = 0.0018$ and its initial external cavity length is $L_2 = 0.16{+}\Delta L_2$ m . ΔL_2 is a small variation. We tested different values of ΔL_2 and observes the changes in SMI waveform. Fig. 6 shows the SMI waveforms when $\Delta L_2 = 4.6111*10^{-8}$ m . The peak to peak value for the no pre-feedback waveform is still 0.8347 and with the pre-feedback is 1.406. The magnified factor is 1.68.

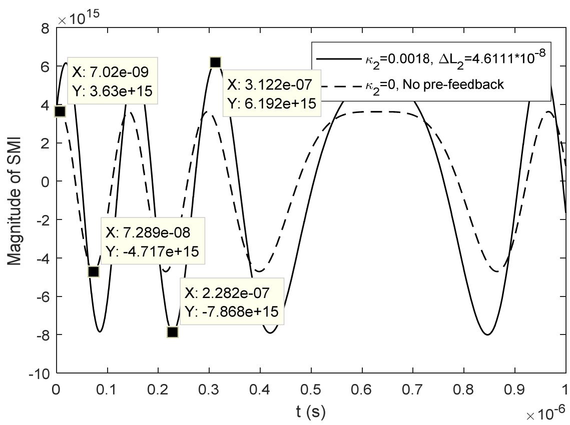

Fig. 6. SMI pre-feedback when $\Delta L_2 = 4.6111*10^{-8}$ m vs SMI without pre-feedback.

Fig. 7 shows the SMI waveforms when $\Delta L_2 = 6.9167*10^{-8}$ m. The peak to peak value for the pre-feedback waveform is 1.98. The magnified factor is 2.37.

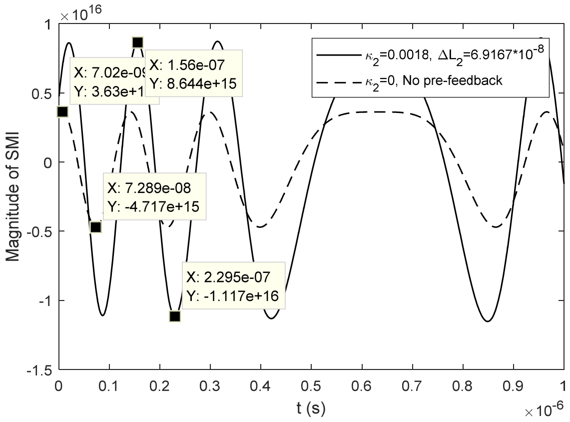

Fig. 7. SMI pre-feedback when $\Delta L_2 = 6.9167*10^{-8}$ m vs SMI without pre-feedback.

Fig. 8 shows the SMI waveforms when $\Delta L_2 = 1.0375*10^{-7}$ m. The peak to peak value for the pre-feedback waveform is 3.251. The magnified factor is 3.89. from above resutls, we can see clearly, the magnitue of the SMI waveform can be further increased with the pre-feedback target located at the proper position.

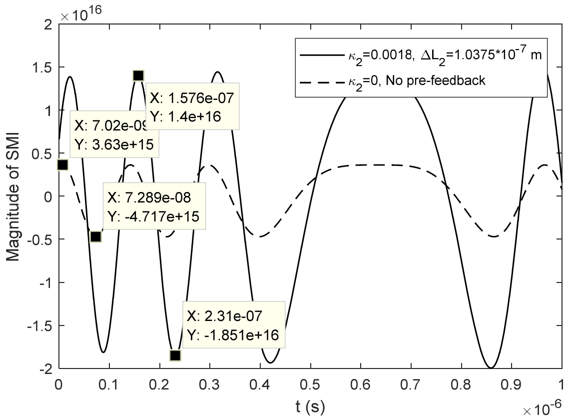

Fig. 8. SMI pre-feedback when $\Delta L_2 = 1.0375*10^{-7}$ m vs SMI without pre-feedback.

3. Experiment

To verify the proposed method, we further built an experimental system as depicted in Fig. 9. The laser emitted by an signle mode LD (Hatachi HL8325G) with wavelength of 830 nm and output power of 40 mW. It is driven and temperature-stabilized by a LD controller (Thorlabs, ITC4001) at the injection current of 60 mA and at the temperature of 23±0.01 ºC. The light emitted by the LD is focused by a lens then passes through a variable attenuator (VA) (Thorlabs, NDC-50C-2M-B) hitted at the measured target (Target-1) which is provided by a white paper attached on a PZT (PI P-841.20).The PZT driven by a PZT controller (PI E-625). The VA is used to adjust the feedback strength for Target-2. Also it acts as the pre-feedback target, because part of the light will be reflected back to the LD. The photodiode (PD) packaged at the rear of the LD is connected to a detection circuit to detect an SMI signal. Finally, the SMI signal is captured and displayed in an oscilloscope.

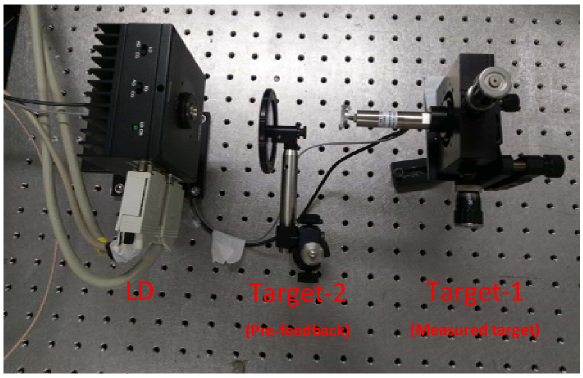

Fig. 9. Experiment Setup.

The experiment started with applying an continious displacement on Target-1. It is controlled by the PZT driver. Adjust the Target-1, make sure a SMI signal can be caputured by the LD. After this, insert VA (Target-2) into the system. At the same time, put a lighttight baffle betweent the VA and Target-1 to block the feedback from Target-1. Set the VA position from the LD as 0.16m, this is the initial external cavity length of the Target-2. Adjust VA to median density, this allows the Target-2 has a stronger feedback strength than Target-1. Then remove the lighttight baffle, allowing the optical feedback from both Target-1 and Target-2 are able to reenter the laser cavity. After this, we can adjust the VA's density from median to high, this increase the feedback strength for pre-feedback. For different pre-feedback strengths, record the corresponding SMI signals with pre-feedback. Last, Slightly adjust the position of Target-2. For different positions, record the corresponding SMI signals.

The experimental results on invesgating the feedback strength influence and target location influence are shown in Fig. 10. Fig. 10(a) is SMI waveform obtained without the presence of Target-2. The SMI signal is very small, this is because the target surface has a very low reflectivity. Once the Target-2 is applied to the system, the SMI signal become visable. This can be seen in Fig. 10(b). Increasing the surface reflectivity by adjusting the VA. The SMI signal magnitude is increased, shown in Fig. 10(c). Then we adjusted the position of the VA. At a certain location, the SMI signal magnitude can reach to a maximum, shown in Fig. 10(d). The peal-peak values in Fig. 10(a), (b), (c) and (d) is about 5 mV, 10 mV, 15 mV and 25 mV respectively. The experiment results show both feedback strength and location of the pre-feedback target can increase the magnitude the SMI signal, this is consistent with the simulation.

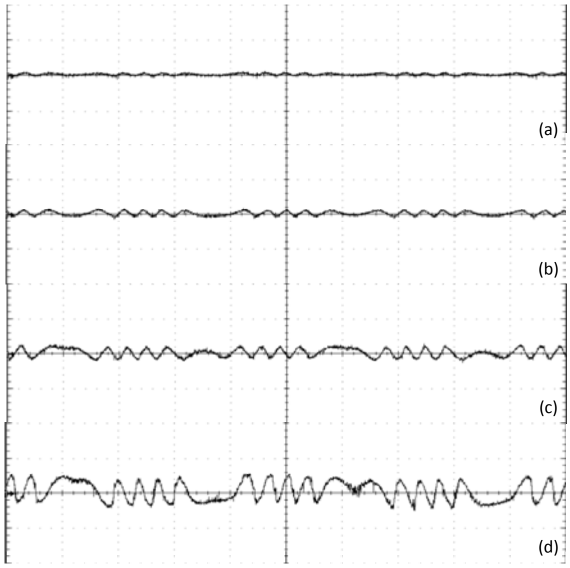

Fig. 10. Experimental result of SMI signal waveforms; (a) SMI signal without pre-feedback. (b) SMI signal with pre-feedback. (c) SMI signal with larger pre-feedback strength. (d) SMI signal with pre-feedback at a location, where the maximum magnitude of the waveform is reached. Scale of X-axis: 1 ms/division, Scale of Y-axix: 50 mV/division.

4. Conclusions

This paper propose to apply a pre-feedback to the SMLD sensor to improve the system sensitivity. Through the simulations and experiment, we verified that both the pre-feedback level and the location of the pre-feedback target can influence the magnitued an SMI signal. By setting a proper pre-feedback, the sensitivity of the SMLD sensor is able to be improved greatly. This bring a useful design idea for desinging a practical SMLD sensor.

References

[1]. S. Donati, G. Giuliani, S. Merlo, Laser diode feedback interferometer for measurement of displacements without ambiguity, *IEEE Journal of Quantum Electronics,* Vol. 31, Issue 1, 1995, pp. 113-119.

[2]. Y. Yu, J. Xi, J. F. Chicharo, Measuring the feedback parameter of a semiconductor laser with external optical feedback, *Optics Express,* Vol. 19, Issue 10, 2011, pp. 9582-9593.

[3]. S. Donati, Developing self-mixing interferometry for instrumentation and measurements, *Laser & Photonics Reviews,* Vol. 6, Issue 3, 2012, pp. 393-417.

[4]. Y. Fan, Y. Yu, J. Xi, J. F. Chicharo, Improving the measurement performance for a self-mixing interferometry-based displacement sensing system, *Applied Optics,* Vol. 50, Issue 26, 2011, pp. 5064-5072.

[5]. B. Liu, Y. Yu, J. Xi, Q. Guo, J. Tong, R. A. Lewis, Displacement sensing using the relaxation oscillation frequency of a laser diode with optical feedback, *Applied Optics,* Vol. 56, Issue 24, 2017, pp. 6962-6966.

[6]. D. Guo, L. Shi, Y. Yu, W. Xia, M. Wang, Micro-displacement reconstruction using a laser self-mixing grating interferometer with multiple-diffraction, *Optics Express,* Vol. 25, Issue 25, 2017, pp. 31394-31406.

[7]. D. Guo, M. Wang, H. Hao, Displacement measurement using a laser feedback grating interferometer, *Applied Optics,* Vol. 54, Issue 31, 2015, pp. 9320-9325.

[8]. M. Norgia, D. Melchionni, A. Pesatori, Self-mixing instrument for simultaneous distance and speed measurement, *Optics and Lasers in Engineering,* Vol. 99, 2017, pp. 31-38.

[9]. S. Shinohara, A. Mochizuki, H. Yoshida, M. Sumi, Laser Doppler velocimeter using the self-mixing effect of a semiconductor laser diode, *Applied Optics,* Vol. 25, Issue 9, 1986, pp. 1417-1419.

[10]. G. Guido, B.-P. Simone, D. Silvano, Self-mixing laser diode vibrometer, *Measurement Science and Technology,* Vol. 14, Issue 1, 2002, p. 24.

[11]. L. Scalise, Y. Yanguang, G. Giuliani, G. Plantier, T. Bosch, Self-mixing laser diode velocimetry: application to vibration and velocity measurement, *IEEE Transactions on Instrumentation and Measurement,* Vol. 53, Issue 1, 2004, pp. 223-232.

[12]. Y. Yanguang, G. Giuliani, S. Donati, Measurement of the linewidth enhancement factor of semiconductor lasers based on the optical feedback self-mixing effect, *IEEE Photonics Technology Letters,* Vol. 16, Issue 4, 2004, pp. 990-992.

[13]. Y. Yu, J. Xi, J. F. Chicharo, T. Bosch, Toward Automatic Measurement of the Linewidth-Enhancement Factor Using Optical Feedback Self-Mixing Interferometry With Weak Optical Feedback, *IEEE Journal of Quantum Electronics,* Vol. 43, Issue 7, 2007, pp. 527-534.

[14]. Y. Yu, J. Xi, Influence of external optical feedback on the alpha factor of semiconductor lasers, *Optics Letters,* Vol. 38, Issue 11, 2013, pp. 1781-1783.

[15]. M. T. Fathi, S. Donati, Thickness measurement of transparent plates by a self-mixing interferometer, *Optics Letters,* Vol. 35, Issue 11, 2010, pp. 1844-1846.

[16]. F. Ross-Conley, K. Bertling, Y. L. Lim, A. P. Bradley, A. D. Rakic, Profiling the change in refractive index using the self-mixing effect in lasers, in *COMMAD 2012*, 2012, pp. 85-86.

[17]. V. Annovazzi-Lodi, S. Merlo, M. Norgia, Measurements on a micromachined silicon gyroscope by feedback interferometry, *IEEE/ASME Transactions on Mechatronics,* Vol. 6, Issue 1, 2001, pp. 1-6.

[18]. T. Bosch, N. Servagent, R. Chellali, M. Lescure, Three-dimensional object construction using a self-mixing type scanning laser range finder, *IEEE Transactions on Instrumentation and Measurement,* Vol. 47, Issue 5, 1998, pp. 1326-1329.

[19]. A. D. Rakić, *et al.*, Swept-frequency feedback interferometry using terahertz frequency QCLs: a method for imaging and materials analysis, *Optics Express,* Vol. 21, Issue 19, 2013, pp. 22194-22205.

[20]. K. Lin, *et al.*, A Fiber-Coupled Self-Mixing Laser Diode for the Measurement of Young's Modulus,

Sensors, Basel, Switzerland, Vol. 16, Issue 6, 2016, p. E928.
[21]. B. Liu, *et al.*, Laser Self-Mixing Fiber Bragg Grating Sensor for Acoustic Emission Measurement, *Sensors,* Vol. 18, Issue 6, 2018, p. 1956.
[22]. J. Perchoux, *et al.*, Current Developments on Optical Feedback Interferometry as an All-Optical Sensor for Biomedical Applications, *Sensors,* Basel, Switzerland, Vol. 16, Issue 5, 2016, p. 694.
[23]. R. Lang, K. Kobayashi, External optical feedback effects on semiconductor injection laser properties, *IEEE Journal of Quantum Electronics,* Vol. 16, Issue 3, 1980, pp. 347-355.